2009

Hyperspectral Reflectance for Rapid Viability Assessment of Bacillus Endospores

Jarrod Edwards
Virginia Commonwealth University

HYPERSPECTRAL REFLECTANCE FOR RAPID VIABILITY ASSESSMENT OF *BACILLUS* ENDOSPORES

A thesis submitted in partial fulfillment of the requirements for the degree of Master of Science at Virginia Commonwealth University.

by

Jarrod Daniel Edwards
Bachelor of Biology
Virginia Commonwealth University
2005

Director: Dr. John Anderson
Associate Professor, Department of Biology

Center for Environmental Studies
Virginia Commonwealth University
Richmond, Virginia
2009

Acknowledgements

I would first and foremost like to thank my family for helping me to become the human being I am today. To my Dad, I'd like to say thanks for the scientific mind and all the support you have given me through college. To Noelle, thanks for putting up with a grumpy meatball and offering guidance and assurance. To Jean Nelson, thank you for all your patience and guidance and infinite wisdom in lab techniques. Garry Glaspell, thanks for letting me ask you questions that other chemists would laugh at me for. Ricky Massaro – big thanks for spending time helping me even though you didn't have any. I couldn't have done it without you. I would like to thank my committee members Dr. Franklin and Dr. Boone for helping me finally find the end of this research. Finally, without the guidance and wisdom of Dr. Anderson I most likely would be shoveling manure or flipping burgers. Thanks, Dude.

Table of Contents **Page**

List of Tables iv

List of Figures v

Abstract vi

Introduction 1

Materials and Methods 7

Endospore Production and Isolation 7

Endospore Killing: Sodium Hypochlorite 7

Endospore Killing: Autoclave 8

Spectral Biomarkers 8

Hyperspectral Analysis 8

Spectral Analysis 9

Spectral Envelope Integration (SEI) 9

Grand Average Integration (GAI) 13

Discrete Support Vector Machine (DSVM) 13

Results 17

SEI 19

GAI 21

DSVM 22

Discussion 24

Spectral Analyses 24

Experimental Conclusions 25

List of Tables **Page**

Summary of Spectral Envelope Integration Results 20

Summary of Grand Average Integration Results 22

List of Figures **Page**

Endospore Diagram 4

Example of Spectral Envelope Integration 11

Example of Grand Average Integration.....13

Example Spectra for *Bacillus megaterium* 16

Example Spectra for *Bacillus subtilis*.....17

Spectral Similarities of Endospores and Protein Powder 18

Abstract

A study was conducted to optically determine the viability of the Gram +, endospore-forming bacterial genera *Bacillus* using a hyperspectral reflectance spectrometer. Endospores are a dormant, differentiated cellular capsule form taken by select bacteria to ensure survival when environmental conditions become unfavorable. Two species of *Bacillus* were used for this study, *Bacillus megaterium* and *Bacillus subtilis*. These endospores were killed using a chemical treatment of sodium hypochlorite or a physical treatment of heat and pressure in an autoclave. The treated samples along with viable samples were lyophilized to form a powder. A reflectance spectrometer measuring 350 nm to 2500 nm (UV to shortwave infrared) was used to collect optical data on bulk powders. The resulting spectra were analyzed using several different methods, including integration and a Support Vector Machine (SVM) to obtain optimal separability of viable and nonviable endospores. Results of this study demonstrated the significant spectral separability of live and dead endospores with a level of confidence <0.05 in both species.

Introduction

Hyperspectral reflectance spectroscopy has played an integral role in remote sensing for over 20 years. Reflectance spectroscopy measures the ratio of reflected radiation of a surface to the total radiation incident on the surface. Hyperspectral reflectance is characterized by many spectral wavelengths possessing narrow bandwidths of 1-5 nm in resolution, depending on the detector, which differs on certain intervals of the total spectrum. In fact, a typical hyperspectral data set is represented by over 300 bands ranging from 350 nm to 2500 nm (ultraviolet through the short-wave infrared). Applications for this type of data acquisition have become wide-ranging and have revolutionized large scale environmental monitoring. Of these applications, critical information has been shown to be resolved concerning plant stress [1-3], marine environments [4-6], and soil/mineral analysis [7-9], among other areas [10].

With regards to microbiological analysis, hyperspectral reflectance has been used to measure mineralogical changes within iron-oxide biofilms produced by acid and circum-neutral gram negative bacteria [11, 12]. While these studies examined the gross precipitates associated with different genera representing the iron bacteria for pollution monitoring, these studies did not associate hyperspectral reflectance with cellular morphologies. Until recently, the use of hyperspectral reflectance has received minimal attention in microbiology for cellular analysis.

While few have studied the reflectance properties of microbes and their respective biomolecular constituents, some studies do exist in several applications. NASA has recently explored hyperspectral reflectance for the determination of extraterrestrial life on

Jupiter's moon Europa using reflectance properties of cryogenically frozen extremophile bacteria [13]. The resulting spectra exhibited portions of biomolecular signatures in the near infrared (NIR) such as proteins, nucleic acids, lipids, and carbohydrates. The results also identified absorptions characteristic of intracellular water at approximately 1.0 µm, 1.25 µm, 1.5 µm, and 2.0 µm. Anderson *et al.* [14] analyzed gross spectral reflectance differences between viable and nonviable endospores in the Visible/NIR (VNIR) region. Although the data obtained in this study only included measurements from 0.4 µm-1.0 µm, spectral differentiation of viable endospores from hydrogen peroxide-treated endospores was achieved.

Finally, hyperspectral/multispectral reflectance has been used effectively in the food industry for rapid detection of contamination. Results from these studies are promising in detecting fecal and cecal contamination, however, no connections are drawn to bacteria and resulting spectral signatures are diluted with organic material that is not of bacterial origin [15-17].

A viable endospore is regarded as capable of germination and formation of a healthy vegetative bacterial cell. Germination is necessary for the reproduction of the bacterium and thus, those incapable of germination are considered nonviable. This irreversible cellular damage is achieved in a number of ways including coat or membrane rupture [18, 19], inactivation of proteins responsible for post-germination spore swelling [20], or irreparable alteration of germination enzyme recognition pathways [21].

The genera *Bacillus* have a unique morphology among their bacterial counterparts. Gram-positive bacteria are characterized as possessing a thick membrane

of peptidoglycan with techoic acids and lacking an outer layer of lipopolysaccharide, present only in Gram-negative bacteria. The distinguishing factor for *Bacillus* lies in their unique ability to form endospores, a characteristic shared by few bacterial genera. An endospore is a dormant, rigid, extremely resistant capsule formed as a survival mechanism. Surrounding a spore's core, which contains its genetic material, are several layers, most notably the cortex, a peptidoglycan barrier and the surrounding spore coat (fig. 1). The spore coat is a complex, multi-layered structure of more than 60 proteins and likely aids in resistance, germination, and enzymatic monitoring of the surrounding environment [22].

Bacteria in the genus *Bacillus* sporulate to form endospores for survival, then germinate and grow when conditions become favorable. There is significant inherent variability in sporulation and germination rates among individual endospores in terms of metabolic potentials. This high degree of variability among individuals enhances species survival during times of extreme change, allowing the community or population as a whole to persist even when the loss of many individuals may occur [18]. When exposed to low doses of decontamination chemicals or sterilants, a certain percentage of endospores within a given population will be more susceptible than others. The rates at which individual active endospores are rendered inactive vary, forming a distribution of viable and nonviable endospores that can fluctuate in accordance with the environment to which they are exposed. For extremely harsh decontamination or sterilizing processes, this distribution is likely to be very narrow. For less severe decontamination procedures

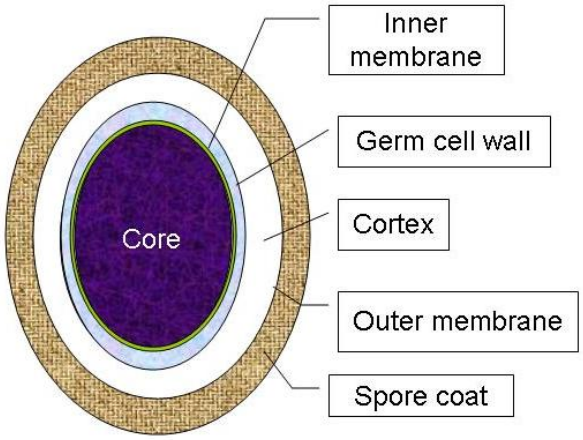

Figure 1. Diagram illustrating the surrounding layers of a bacterial endospore of the genus *Bacillus*.

the distribution is likely to become much broader. Severe decontamination agents such as paraformaldehyde [23] or methyl bromide [24] have unacceptable environmental impacts and therefore have limited use and are strictly regulated by the EPA.

The minimal metabolic activity endospores exhibit [25, 26] severely limits efforts to target metabolic processes in viability testing. The spore coat and membrane, however, may be a good indication of whether a spore is alive or not. Endospore membranes allow for differentiation stains with fluorescent dyes [27] and, given sufficient time and controlled conditions, subtle differences in membrane permeability can be detected. Fluorescent dyes have been used to differentiate live from dead endospores, but these preparations often yield a preponderance of bacterial endospores that appear as somewhere between alive and dead. In addition, use of fluorescent dyes in environmental applications has limitations due to isolation and preparation of samples. Although the use of fluorescent microscopy to evaluate endospore viability shows promise, error associated with current methodologies has precluded collective adoption of these techniques for use in real world situations.

Currently there exists no rapid, optically-based means to differentiate viable bacterial endospores from those that are nonviable. Germination, or the beginnings of growth in *B. anthracis* and other bacterial endospores, is required before genes essential for infection are transcribed and the likelihood of disease is increased [25]. Therefore, a rapid and quantitative assessment of whether an endospore is alive (viable), and thus possesses the potential to germinate is prerequisite to establishing health risks following an exposure or to ascertain efficacy of sterilization procedures. Current and accepted

methods for determining endospore viability require growth on microbiological media, which takes days for verification due to the time requirement for growth to ensue. Micro- and nano-sensor technologies show promise as a means of optically confirming bacterial presence, but have not been shown to possess the ability to distinguish between viable and nonviable spores [28-31]. Scatter and depolarization signatures from polarized laser sources can be used to quantify aerosol particle size and shape and to infer an endospore presence [32, 33], however, these technologies do not provide information on endospore viability.

The hypotheses for this research are that 1) rapid differentiation of viable and nonviable endospores is achievable through analysis of hyperspectral reflectance data and 2) that these changes are due to decontamination-induced effects of the spore coat.

Methods

Endospore Production and Isolation

Two species of *Bacillus* were obtained from Virginia Commonwealth University, *B. megaterium* and *B. subtilis*. Cultures were heat shocked at 100°C for 60 seconds to trigger germination and immediately streaked on Tryptic Soy Agar (TSA), while malachite green endospore staining and Gram-stain methods were utilized to ensure successful isolation. Isolated colonies were used to inoculate sterile Schaeffer's sporulation broth [34] and incubated with shaking at 30°C for 72 hrs. Samples were centrifuged at 7,000 rpm for 5 minutes to remove the cells from the medium then resuspended in Phosphate Buffered Solution (PBS). After samples were allowed to sporulate for 3 weeks, the samples were washed with sterile DI water several times prior to killing treatments. All samples were lyophilized with a Labconco FreeZone 2.5 (Labconco, Corp., Kansas City, MO) to form light, fluffy spore material.

Endospore Killing: Sodium Hypochlorite - Bleach

Household bleach was diluted to 20% for treatments and gently mixed with endospores for 1 hour. Samples were then rinsed with sterile DI water and centrifuged at 7,000 rpm for 5 minutes to form a pellet. This rinsing was repeated 2 additional times. Streak plates confirmed the absence of viable spores. These treated spore suspensions were then lyophilized for 24 hours.

Endospore Killing: Autoclave

Endospores were autoclaved for 90 minutes at a temperature and pressure of 121°C and 15 psi to ensure complete kill. Streak plates confirmed the absence of viable spores. These spore suspensions were then lyophilized for 24 hours.

Spectral Biomarkers

In consideration of the proteinaceous makeup of the spore coat, the reflectance of whey protein powder was measured. Whey protein consists of several different proteins, which may spectrally mimic the variety found in the spore coat. The spectrum of protein powder, if similar to the signature of endospores, may help to confirm that absorption characteristics observed in the spectra of endospores is due to protein.

Hyperspectral Analysis

The instrument used for spectroscopic measurements in this study was a FieldSpec® Pro reflectance spectrometer manufactured by Analytical Spectral Devices Inc. (ASD). The spectral range and resolution is 350 nm to 2500 nm in over 300 bands at 1 to 5 nm.

Measurements were carried out in a Class 2 Laminar Flow Hood for safety purposes (i.e. limit aerosolized airborne endospore material). A 3200 K color Lowel Tota-Light (tungsten) was used to illuminate the samples. This lamp effectively provides a continuous spectrum similar to that of the Sun. Reflectance spectra were collected using a white NIST (National Institute of Standards and Testing) reflectance standard (halon), first as a normalization calibration for the instrument and later as a background for each measurement. Measurements of samples were also obtained using a 50% grey

NIST standard and flat black as backgrounds. The mean of five spectra was obtained from each treated (nonviable) and untreated (viable) sample to provide a representative spectrum from the entire surface of the samples. Each sample consisted of a layer of endospores distributed in Petri dishes. The true Field-of-View (FOV) was calculated to be 0.722 mm^2 (using the instrument's 8° FOV) at a distance of 4.70 cm, at nadir viewing geometry.

Spectral Analysis

Two methods were employed to analyze the spectra of both viable and nonviable spores. The specific area of interest (AOI) was a 70 nm window between 380 nm and 450 nm. This AOI was chosen for two reasons: 1) a preliminary visual characterization of consistent changes in absorption in this area due to treatment and 2) a priori knowledge of fluorescence absorptions of biomolecular aromatic amino acids to be in the area of 350 nm to 450 nm. A smoothing function was applied to the spectra prior to analysis, using a wavelet algorithm by chemometric software, ParLes [35]. Three analytical methods were used to quantify the observed spectral differences between live and dead endospores: Spectral Envelope Integration (SEI), Grand Average Integration (GAI), and Discrete Support Vector Machine (DSVM) methods.

Spectral “Envelope” Integration (SEI)

A hypothetical enclosure to the absorption in the AOI was created by calculating a line between the reflectance values at 380 nm and 450 nm (Fig. 2). This method was used effectively in previous studies involving chlorophyll content in plants [36] and adapted for use in the current study. The spectral “envelope” and the integral of the resulting space were determined using the following equations:

$$(1.1)\ SE = \left(\frac{R_f - R_i}{\lambda_{TOT}}\right)\lambda_j + \left(R_j - \left(\frac{R_f - R_i}{\lambda_{TOT}}\right) * 380\right),$$

where R_f is the reflectance value at 450 nm and R_i is the reflectance value at 380 nm. The size of the AOI in nanometers is represented by λ_{TOT}, the specific wavelength is λ_j and R_j is the reflectance value at that specific wavelength. The integral calculated using this spectral envelope was calculated with the equations:

$$(1.2)\ SEI = \int_{380}^{450} R_{ED},$$

where

$$(1.3)\ R_{ED} = (F(s) - F(i))d\lambda,$$

where $F(s)$ is the function of the spectral envelope and $F(i)$ is the function of each individual sample spectrum. These integrals were calculated numerically as opposed to analytically.

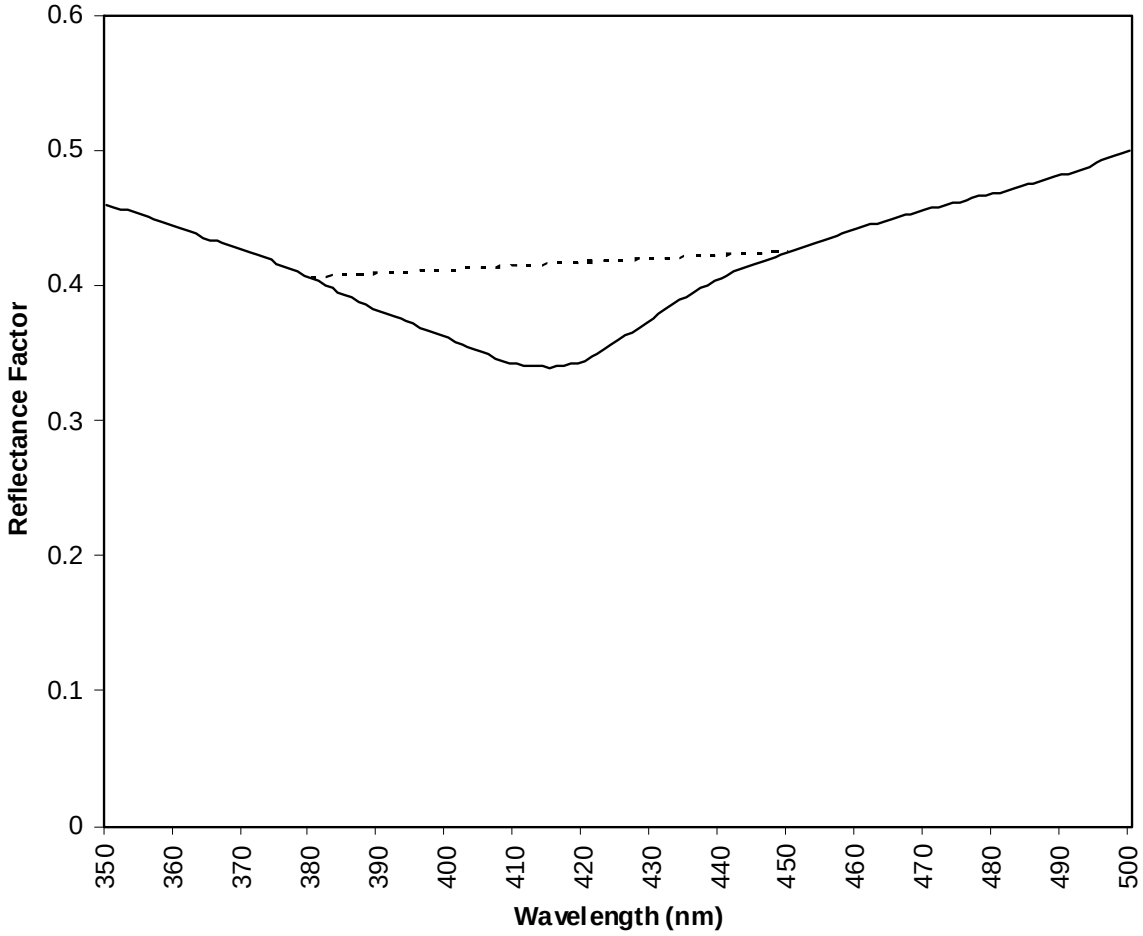

Figure 2. This is an example of the Spectral Envelope Integration (SEI) method. The solid line represents an individual sample spectrum and the broken line denotes the spectral envelope (SE).

Grand Average Integration (GAI)

All sample data were shifted to a 0.3 reflectance value at 380 nm. A spectrum was created by averaging all sample data, both treated and untreated, in the AOI. This was used to calculate the integrals and thus, determine the area between each sample spectrum and the "grand average" spectrum using the following equation:

$$(1.4)\ GAI = \int_{380}^{450} (F(i) - \overline{F}(i)) * -1,$$

where $F(i)$ represents the individual sample spectrum and $\overline{F}(i)$ is the average of all sample spectra. This equation created an environment where values below the grand average had negative values and those above had positive values as shown in Figure 3**.**

Discrete Support Vector Machine (DSVM)

The support vector machine (SVM) used is a supervised learning method for binary classification of data via mathematical optimization. This method analyzes data as two sets of vectors in n-dimensional space. Data are projected into a higher-dimensional space in which a hyperplane is created that separates and maximizes the margin between the data sets, corresponding to a nonlinear separating surface in the space of the original data. SVM with the ramp loss [37] has been shown to provide robustness properties in the presence of outlier observations.

The SVM instances are trained and tested using the ramp loss as described in [37] on machines with a 2.6 GHz Opteron processors and 2 GB RAM. The training of models is limited to 10 minutes (600 CPU seconds). If after 10 minutes a globally-optimal solution is not found, the best known solution is used. SVM is trained using a training

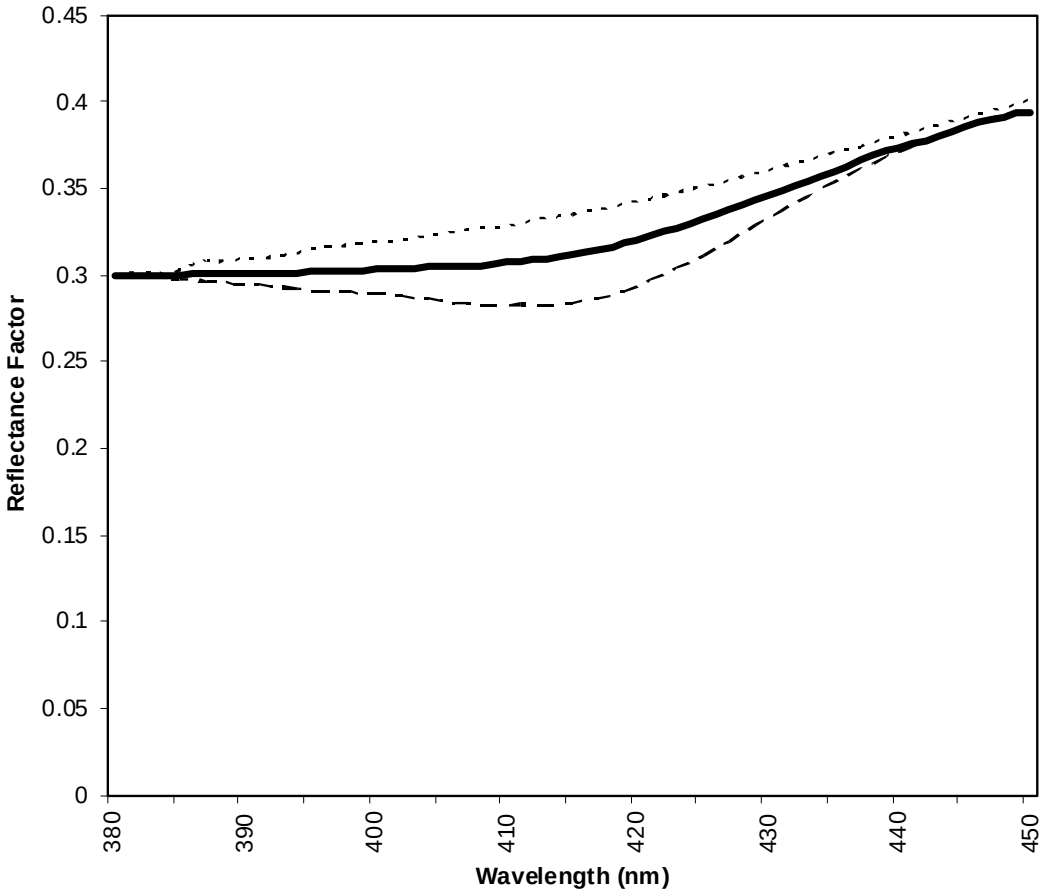

Figure 3. This is an example of the Grand Average Integration (GAI) method. The bold spectrum represents the "grand average" spectrum. The broken lines are examples of sample spectra. Integrals calculated for spectra below the grand average had negative values while those above had positive values.

data set for various settings including choice of kernel (linear, degree-2 polynomial, degree-9 polynomial, and Gaussian), the parameter C that represents the tradeoff between misclassification error and regularization (0.01, 0.1, 1, 10, 100), and the parameter gamma that represents the width of the Gaussian kernel (0.1, 1, 10, 100, 1000). The best-performing combination of settings on the validation set is then applied to the test set, for which results are reported.

The spectral data acquired in this study were tested with the DSVM in two ways. The first test incorporated all the data (236 observations), including all backgrounds and treatments of both species of *Bacillus* with the intention of differentiating viable and nonviable endospores. The second and third tests were separated by treatment (autoclave or bleach-treated) and compared each treatment to viable spores including all measurement backgrounds (160 observations for each test). In each scenario, the measurements were randomly partitioned into a training set (50% of test spectra), a validation set (25% of test spectra), and a test set (25% of test spectra).

Results

The sample sizes in both SEI and GAI analyses varied. For *B. subtilis* on a white background, the sample sizes for live, bleach-treated, and autoclave-treated were 11, 10, and 11, respectively. For *B. megaterium* on a white background, the sample sizes for all treatments were 19. In measurements taken using both grey and black backgrounds the sample sizes for each treated and untreated group of *B. subtilis* and *B. megaterium* were 10 and 15, respectively. As stated previously, five spectra were obtained for each sample and an average was then calculated yielding a single spectrum that was representative of the entire sample surface (Fig. 4, 5).

Comparison of spore spectra and that of whey protein yielded surprising results. The absorption characteristics observed were strikingly similar. In fact, most major absorptions present in the signatures of endospores were very close to those of whey protein powder. Nearly all absorptions, not linked with intracellular water, that were present in both the spectra of endospores and protein powder have been linked to the harmonics and overtones of molecular vibrations due to bending and stretching of strong bonds associated with proteins. Examples of major absorptions present in endospores were at 1510 nm which is associated with the 1st overtone of an N-H stretch in proteins, and 2060 nm which is linked to the 2nd overtone of an N=H bend in proteins [37], to name just a few (Fig. 6).

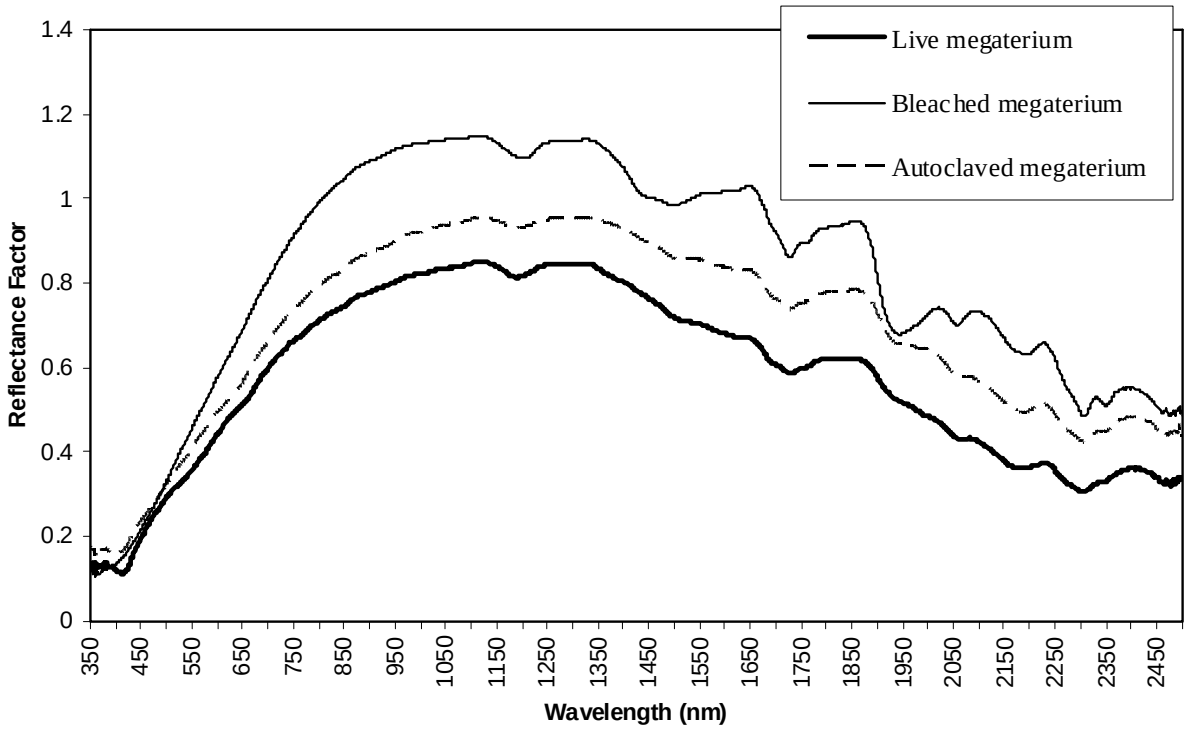

Figure 4. Example spectra for treated and non-treated spores of *B. megaterium*. Each sample spectrum consists of an average of five spectra, representative of the entire sample surface. Live spores exhibit deeper absorption in the area of interest (AOI) (380nm-450nm) than both autoclave-treated and bleach-treated spores.

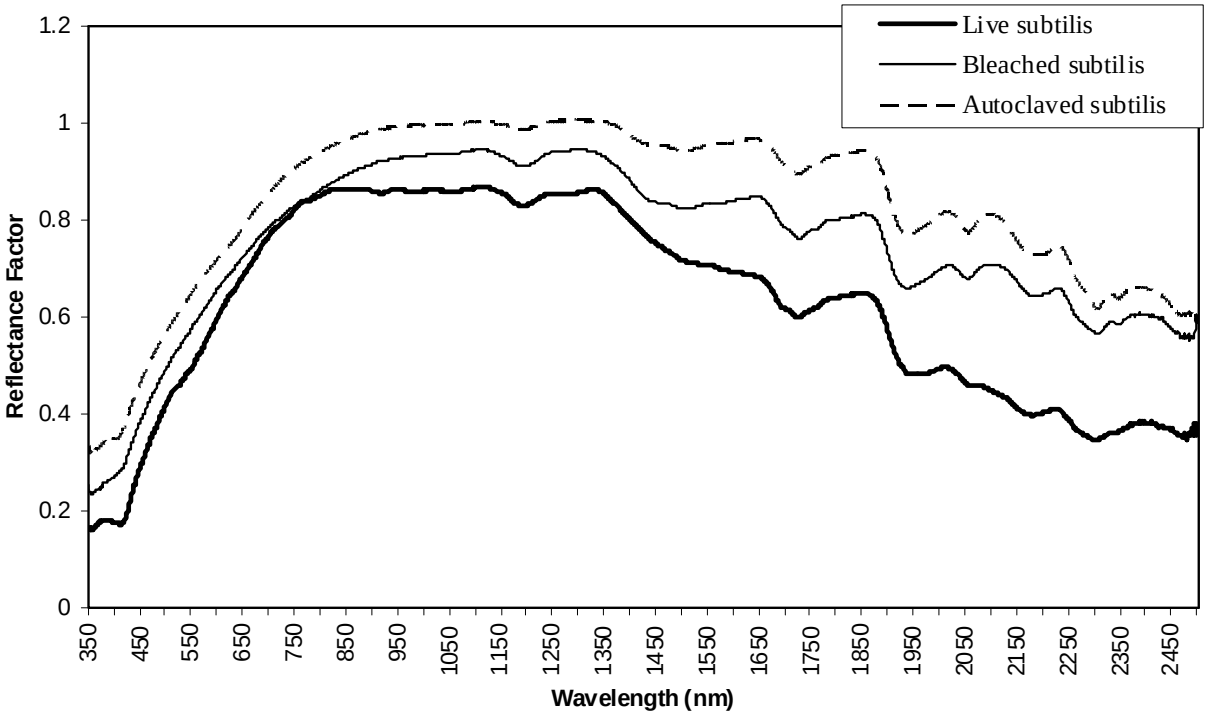

Figure 5. Example spectra for treated and non-treated spores of *B. subtilis.* Each sample spectrum consists of an average of five spectra, representative of the entire sample surface.

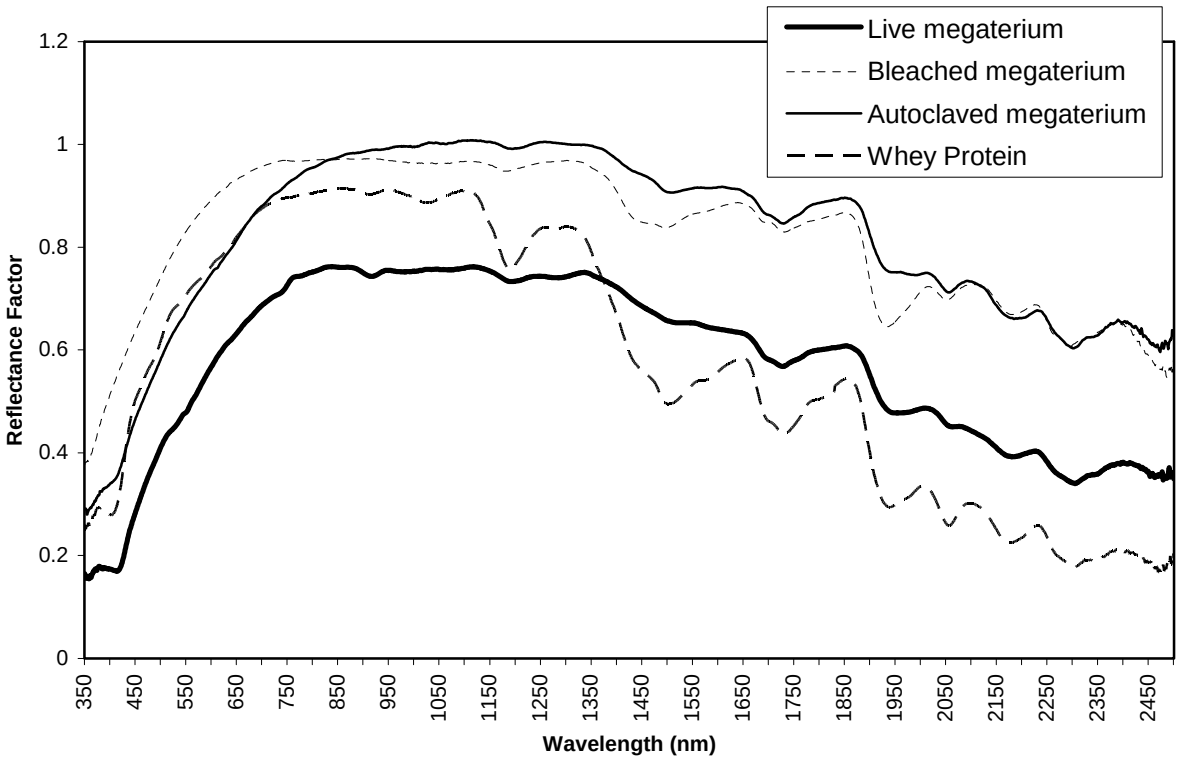

Figure 6. Similarities in reflectance absorptions between whey protein powder and both treated and untreated endospores. Identical absorptions are found at 410 nm, 910 nm, 1020 nm, 1510 nm, 1690 nm, 2060 nm, and throughout the short-wave infrared (SWIR).

Spectral Envelope Integration (SEI)

The SEI method yielded significant spectral separation of live and dead *Bacillus* endospores. Respective integral means for *B. subtilis* measured against a white background were 2.364, 0.821, and 0.946 for live, bleach-treated, and autoclave-treated spores. Means for *B. subtilis* against a grey background were 2.289, 0.618, and 0.838 while those against a black background were 1.899, 0.487, and 0.740, respectively. Means for *B. megaterium* measured against a white background were 2.328, 0.492, and 1.117 for live, bleach-treated, and autoclave-treated spores. Means for *B. megaterium* measured against a grey background were 2.087, 0.401, and 0.925 while those against a black background were 1.923, 0.305, and 0.903, respectively. The integrals calculated for samples measured against a white background were normally distributed allowing a One Way ANOVA to be used to analyze the results with a Tukey's test for pairwise comparison using SigmaStat 3.5 software. For samples measured against either a grey or black background the integral distributions were normal but lacked equal variance, requiring a nonparametric Kruskal-Wallis on ranks and Dunn's method for pairwise comparisons.

Both *B. subtilis* and *B. megaterium* showed a high degree of separation between the reflectance spectra of live endospores to those killed by either treatment when measured against both a white and grey background. The integrals within the spectral envelope between live and dead *B. subtilis* spores against a white background were significantly different at a level of confidence (p-value) of <0.001, regardless of treatment. The same level of confidence was found between live and dead spores of *B.*

megaterium against a white background. For samples measured against a grey background, p-values of <0.05 were found between live and dead spores of both species, regardless of treatment (Table 1).

Measurements against a dark background using SEI demonstrated less sensitivity in comparison to lighter backgrounds. All comparisons between live and dead of either species were significant at a p <0.05 with the exception of live spores of *B. megaterium* compared with those that were autoclave-treated (p >0.05).

Table 1. SEI analysis pairwise comparisons for level of significance (p) between integrals of viable and nonviable *Bacillus*. Tukey's test is associated with a parametric ANOVA while Dunn's test is associated with a nonparametric Kruskal-Wallis test on ranks.

Comparison	**Background**	**Pairwise Test**	**P<0.05**
Bacillus subtilis			
Live vs. Bleached	White	Tukey's	Yes
Live vs. Autoclaved	White	Tukey's	Yes
Live vs. Bleached	Grey	Dunn's	Yes
Live vs. Autoclaved	Grey	Dunn's	Yes
Live vs. Bleached	Black	Dunn's	Yes
Live vs. Autoclaved	Black	Dunn's	Yes
Bacillus megaterium			
Live vs. Bleached	White	Tukey's	Yes
Live vs. Autoclaved	White	Tukey's	Yes
Live vs. Bleached	Grey	Dunn's	Yes
Live vs. Autoclaved	Grey	Dunn's	Yes
Live vs. Bleached	Black	Dunn's	Yes
Live vs. Autoclaved	Black	Dunn's	No

Grand Average Integration

The GAI analysis also displayed significant separation in the spectra of live and dead spores. Respective integral means for *B. subtilis* against a white background for live, bleach-treated, and autoclave-treated spores were -0.936, 1.601, and 0.086. Means for *B. subtilis* against a grey background were -1.111, 1.769, and 0.479 while those against a black background were -0.970, 1.481, and 0.569, respectively. Means for *B. megaterium* against a white background were 2.007, 2.049, and -0.432, respectively. Means for *B. megaterium* against a grey background were -1.561, 1.154, and -0.351 while those measured against a black background were -1.372, 0.951, and -0.299, respectively. Integrals calculated against a grand average, as opposed to the spectral envelope, lacked normality as a dataset. It was then necessary to use a nonparametric Kruskal-Wallis test on ranks combined with Dunn's method for pairwise comparison using SigmaStat 3.5 software (table 2).

Reflectance spectra of viable and nonviable *B. megaterium* were highly differentiable when measured against a white background. Both bleached and autoclaved spores were significantly different from live spores ($p < 0.05$). Bleached spores were also differentiable from autoclaved spores of *B. megaterium* with $p<0.05$. All comparisons between live and dead spores measured against both grey and black backgrounds were significant at $p < 0.05$ except live versus autoclaved spores of *B. megaterium*, which had $p > 0.05$.

Spores of *B. subtilis* were also separable spectrally. Live spores differed significantly from bleached spores at $p<0.05$ among this species. Strangely, live *subtilis*

were not different from those that were autoclave-treated when measured against a white background but when measured against either grey or black backgrounds, demonstrated significance at $p < 0.05$.

Table 2. GAI analysis pairwise comparisons for level of significance (p) between integrals of viable and nonviable *Bacillus*. Tukey's test is associated with a parametric ANOVA while Dunn's test is associated with a nonparametric Kruskal-Wallis test on ranks.

Comparison	Background	Pairwise Test	P<0.05
Bacillus subtilis			
Live vs. Bleached	White	Dunn's	Yes
Live vs. Autoclaved	White	Dunn's	No
Live vs. Bleached	Grey	Dunn's	Yes
Live vs. Autoclaved	Grey	Dunn's	Yes
Live vs. Bleached	Black	Dunn's	Yes
Live vs. Autoclaved	Black	Dunn's	Yes
Bacillus megaterium			
Live vs. Bleached	White	Dunn's	Yes
Live vs. Autoclaved	White	Dunn's	Yes
Live vs. Bleached	Grey	Dunn's	Yes
Live vs. Autoclaved	Grey	Dunn's	No
Live vs. Bleached	Black	Dunn's	Yes
Live vs. Autoclaved	Black	Dunn's	No

Discrete Support Vector Machine (DSVM)

Binary classification of viable and nonviable spores was achieved using DSVM. Optimal settings were found to be common among all three tests using a Gaussian kernel, a value of 100 for parameter C, and a value of 1 for parameter gamma. The test incorporating all the data, regardless of treatment, resulted in a confusion matrix that

misclassified 2 observations out of 22 viable spores as nonviable and 4 out of 38 nonviable spores as viable, yielding a final accuracy of 90%. The test comparing autoclave-treated and viable spores returned a confusion matrix that misclassified 1 observation in a total of 20 viable spores as noviable and 2 in 20 nonviable spores as viable, with a final calculated accuracy of 92.5%. Finally, the test between bleach-treated and viable spores, resulted in a confusion matrix that misclassified only 1 observation in 24 viable spores as nonviable and 0 out of 16 nonviable as viable, for a final accuracy of 97.5%.

Discussion

Spectral Analyses

Two analytical methods involving spectral integration were used in this study. The spectral envelope method (SEI) [36] measured the area of the desired absorption using an "envelope" applied to each individual spectrum in the AOI. Since the spectrometer is normalized prior to measurements using a halon standard, this approach was used on the assumption a second normalization may be unnecessary. After all, the phenomenon in the AOI was more dependent on the amplitude of individual absorptions rather than relative reflectance intensity. The grand average method (GAI), by contrast, applied a second normalization to each measurement. In this approach, spectra were normalized to 0.3 reflectance factor and the area was compared between each individual spectrum and an average of all the measurements collected as a constant reference. This method was more constant in regard to analytical parameters (i.e. y-intercept, integration against a constant average spectrum).

Although both methods yielded significant results, the spectral envelope method demonstrated greater separability between viable and nonviable endospores. The reasoning behind this difference could be due to a loss of power due to the use of nonparametric Kruskal-Wallis tests on ranks for all GAI analyses.

The Discrete Support Vector Machine (DSVM) also demonstrated significant differentiation among viable and nonviable endospores. Binary classification as simply "live" or "dead" was achieved at 90% accuracy among all data, regardless of treatment or background. This accuracy improved significantly when the tests were separated by

treatment. Bleach-treated spores were separable from viable spores at 97.5% accuracy, displaying the most significant separability among the two treatments.

The use of DSVM for binary classification is useful in the present application for several reasons. It allows for a very rapid assessment of whether the interrogated threat of infection by endospores is high or minimized with a simple classification of "live" or "dead". In addition, little to no pretreatment is necessary for this analysis to yield accurate results. In this respect, use of DSVM in real-world field applications could prove a powerful tool in viability classification of *Bacillus* endospores.

Experimental Conclusions

This research has demonstrated a rapid optical method for the differentiation of viable and nonviable endospores in two different species of *Bacillus* on various backgrounds using reflectance spectroscopy. In comparing the results in respect to the backgrounds, it appeared the black background consistently yielded slightly less significant results. This could be due to lower overall reflectance values associated with a dark surface and the subsequent loss of depth in the absorption features.

A spectral absorption at 420 nm has been consistently measured that remains significant in the spectra of live spores but tends to become shallow upon treatment by both bleach and autoclaving. This shallowing is visually apparent and statistically significant when analyzed using integrals in the AOI. It remains a strong possibility that this absorption is due to a biomolecular alteration in the outermost layer of the endospore, the spore coat. Recent research determined that bleach causes significant oxidative damage to the coat protein [19]. Similar findings have been discovered on irreversible

heat denaturation of proteins [38, 39] and membrane/cortex of *Bacillus* [40]. However, research concerning optical characteristics of biomolecules with regard to microbes is scarce. Taking into consideration the proteinaceous makeup of the spore coat, it seems a reasonable assumption that much of what is seen in the reflectance spectra of endospores are proteins. Furthermore, the reflectance characteristics of one protein may not be representative of an agglomeration of proteins, which is closer to the structure of the spore coat.

To explore this possibility, the reflectance of whey protein powder was measured. Whey protein powder is a collection of globular proteins that is isolated from whey, a by-product of cheese. The spectral absorptions of this collection of proteins were strikingly similar to those seen in the spectra of both viable and nonviable *Bacillus* endospores. The absorption minimum of whey protein at ~410 nm is extremely close to the absorption still prominent in live endospores at ~418 nm, which many may regard to be negligible in difference. These findings in conjunction with the similarities between absorptions due to molecular vibrations due to proteins [37] and observed spectra in spores further strengthen the argument that the observed spectra of endospores is due to protein.

An abundance of research has focused on the degradation of protein by a variety of mechanisms. It is well-established that proteins and many other biomolecules demonstrate high reactivity in the presence of hypochlorite. Hawkins *et al*. reviewed both the mechanisms and kinetics of the oxidation of proteins by hypochlorite and highlighted the initial oxidation of side chains and subsequent attack of secondary chloramine intermediates. Their review, along with other research, cited that oxidative

attack on proteins is very likely to result in enzyme inhibition and/or loss of structural function [41, 42]. The application of heat to proteins is also known to denature conformational structure of proteins as well as destroy functionality [38, 39]. This finding furthers the argument that the degradation of protein by oxidation or denaturing by heat may explain the change in absorption in our AOI.

It is likely that the degradation of the proteins in the spore coat is not the sole explanation for the death of the endospore. Several studies have pointed to the spore membrane as the cause of inactivation by oxidation in *Bacillus* [19, 43]. In order to use spore coat integrity as an indicator of viability it would be helpful to determine the rates at which the spore components are denatured and the lag time between these events, in addition to further research concerning the optical characteristics associated with intact and degraded coat proteins in bacterial endospores.

References

1. Pietrzykowski, E., et al., Predicting Mycosphaerella leaf disease severity in a Eucalyptus globulus plantation using digital multi-spectral imagery. Southern Hemisphere Forestry Journal, 2007. **69**(3): p. 175-182.
2. Zarco-Tejada, P.J., C.A. Rueda, and S.L. Ustin, Water content estimation in vegetation with MODIS reflectance data and model inversion methods. Remote Sensing of Environment, 2003. **85**(1): p. 109-124.
3. Milton, N.M., et al., Arsenic-induced and selenium-induced changes in spectral reflectance and morphology of soybean plants. Remote Sensing of Environment, 1989. **30**(3): p. 263-269.
4. Baban, S.M.J., Environmental monitoring of estuaries estimating and mapping various environmental indicators in Breydon Water Estuary, UK, using Landsat TM imagery. Estuarine Coastal and Shelf Science, 1997. **44**(5): p. 589-598.
5. Snyder, W.A., et al., Optical scattering and backscattering by organic and inorganic particulates in US coastal waters. Applied Optics, 2008. **47**(5): p. 666-677.
6. Alparslan, E., et al., Water quality assessment at Omerli Dam using remote sensing techniques. Environmental Monitoring and Assessment, 2007. **135**(1-3): p. 391-398.
7. Stenberg, B.O., E. Nordkvist, and L. Salomonsson, Use of near-infrared reflectance spectra of soils for objective selection of samples. Soil Science, 1995. **159**(2): p. 109-114.
8. Bell, J.F. and T.M. Ansty, High spectral resolution UV to near-IR observations of Mars using HST/STIS. Icarus, 2007. **191**(2): p. 581-602.
9. Wu, Y.Z., et al., Feasibility of reflectance spectroscopy for the assessment of soil mercury contamination. Environmental Science & Technology, 2005. **39**(3): p. 873-878.
10. Foley, W.J., et al., Ecological applications of near infrared reflectance spectroscopy a tool for rapid, cost-effective prediction of the composition of plant and animal tissues and aspects of animal performance. Oecologia, 1998. **116**(3): p. 293-305.
11. Anderson, J.E. and E.I. Robbins, Spectral reflectance and detection of iron-oxide precipitates associated with acidic mine drainage. Photogrammetric Engineering and Remote Sensing, 1998. **64**(12): p. 1201-1208.
12. Robbins, E.I., J. Anderson, M.H. Podwysocki, and G. Nord, Seasonal Variations in Spectral Reflectance of Microbial Flocculates, Precipitates, and Oil-like films Associated with Neutral and Acid Mine Drainage, in Environmental Monitoring and Biodiagnostics of Hazardous Contaminants, M.H.e. al, Editor. 2002, Kluwer Academic Publishers. p. pp.243-266.
13. Dalton, J.B., et al., Near-infrared detection of potential evidence for microscopic organisms on Europa. Astrobiology, 2003. **3**(3): p. 505-529.

14. Anderson J., C.R., D. Ringelberg, J. Edwards, K. Foley, Differentiation of Live-Viable versus Dead Bacterial Endospores by Calibrated Hyperspectral Reflectance Microscopy. Journal of Microsopy, 2008. **Accepted paper**.
15. Gowen, A.A., et al., Hyperspectral imaging - an emerging process analytical tool for food quality and safety control. Trends in Food Science & Technology, 2007. **18**(12): p. 590-598.
16. Liu, Y.L., et al., Development of simple algorithms for the detection of fecal contaminants on apples from visible/near infrared hyperspectral reflectance imaging. Journal of Food Engineering, 2007. **81**(2): p. 412-418.
17. Park, B., et al., Performance of hyperspectral imaging system for poultry surface fecal contaminant detection. Journal of Food Engineering, 2006. **75**(3): p. 340-348.
18. Margosch, D., et al., Pressure inactivation of Bacillus endospores. Applied and Environmental Microbiology, 2004. **70**(12): p. 7321-7328.
19. Young, S.B. and P. Setlow, Mechanisms of killing of Bacillus subtilis spores by hypochlorite and chlorine dioxide. Journal of Applied Microbiology, 2003. **95**(1): p. 54-67.
20. Melly, E., A.E. Cowan, and P. Setlow, Studies on the mechanism of killing of Bacillus subtilis spores by hydrogen peroxide. Journal of Applied Microbiology, 2002. **93**(2): p. 316-325.
21. Setlow, B., et al., Mechanisms of killing spores of Bacillus subtilis by acid, alkali and ethanol. Journal of Applied Microbiology, 2002. **92**(2): p. 362-375.
22. Driks, A., The Bacillus spore coat. Phytopathology, 2004. **94**(11): p. 1249-1251.
23. EPA, U. Antrax spore decontamination using paraformaldehyde. 2007 [cited 2009 March 20]; Available from: http://www.epa.gov/opp00001/factsheets/chemicals/paraformaldehyde_factsheet.htm.
24. EPA, U. Anthrax spore decontamination using methyl bromide. [Internet] 2007 July 2007 [cited 2009 March 20]; Available from: http://www.epa.gov/opp00001/factsheets/chemicals/methylbromide_factsheet.htm .
25. Liu, H.B., et al., Formation and composition of the Bacillus anthracis endospore. Journal of Bacteriology, 2004. **186**(1): p. 164-178.
26. Atrih, A. and S.J. Foster, Bacterial endospores the ultimate survivors. International Dairy Journal, 2002. **12**(2-3): p. 217-223.
27. Laflamme, C., et al., Assessment of bacterial endospore viability with fluorescent dyes. Journal of Applied Microbiology, 2004. **96**(4): p. 684-692.
28. Setkus, A., et al., Qualitative and quantitative characterization of living bacteria by dynamic response parameters of gas sensor array. Sensors and Actuators B-Chemical, 2008. **130**(1): p. 351-358.
29. Miyano, K., et al., Rapid and highly sensitive detection of bacteria sensor using a porous ion exchange film. Japanese Journal of Applied Physics, 2008. **47**(4): p. 3240-3243.

30. Zhou, Y.X., B. Yu, and K. Levon, Potentiometric sensor for dipicolinic acid. Biosensors & Bioelectronics, 2005. **20**(9): p. 1851-1855.
31. Taylor, L.C., M.B. Tabacco, and J.B. Gillespie, Sensors for detection of calcium associated with bacterial endospore suspensions. Analytica Chimica Acta, 2001. **435**(2): p. 239-246.
32. Venkatapathi, M., et al., High speed classification of individual bacterial cells using a model-based light scatter system and multivariate statistics. Applied Optics, 2008. **47**(5): p. 678-686.
33. Duncan, D.D. and M.E. Thomas, Particle shape as revealed by spectral depolarization. Applied Optics, 2007. **46**(24): p. 6185-6191.
34. Harwood, C., ed. Molecular Biological Methods for Bacillus. ed. S. Cutting. 1990, John Wiley & Sons, Inc.: New York.
35. Rossel, R.A.V., ParLeS: Software for chemometric analysis of spectroscopic data. Chemometrics and Intelligent Laboratory Systems, 2008. **90**(1): p. 72-83.
36. Oppelt, N. and W. Mauser, Hyperspectral monitoring of physiological parameters of wheat during a vegetation period using AVIS data. 2004: p. 145-159.
37. Curran, P.J., REMOTE-SENSING OF FOLIAR CHEMISTRY. Remote Sensing of Environment, 1989. **30**(3): p. 271-278.
38. Le Bon, C., T. Nicolai, and D. Durand, Kinetics of aggregation and gelation of globular proteins after heat-induced denaturation. Macromolecules, 1999. **32**(19): p. 6120-6127.
39. Yadav, S. and F. Ahmad, A new method for the determination of stability parameters of proteins from their heat-induced denaturation curves. Analytical Biochemistry, 2000. **283**(2): p. 207-213.
40. Belliveau, B.H., et al., Heat killing of bacterial-spores analyzed by differential scanning calorimetry. Journal of Bacteriology, 1992. **174**(13): p. 4463-4474.
41. Hawkins, C.L., D.I. Pattison, and M.J. Davies. Hypochlorite-induced oxidation of amino acids, peptides and proteins. 2003: Springer-Verlag.
42. Nalian, A. and A.V. Iakhiaev, Possible mechanisms contributing to oxidative inactivation of activated protein C: Molecular dynamics study. Thrombosis and Haemostasis, 2008. **100**(1): p. 18-25.
43. Cortezzo, D.E., et al., Treatment with oxidizing agents damages the inner membrane of spores of Bacillus subtilis and sensitizes spores to subsequent stress. Journal of Applied Microbiology, 2004. **97**(4): p. 838-852.